Auger transition rates for excitons bound to acceptors in Si and Ge†

G. C. Osbourn and D. L. Smith
California Institute of Technology, Pasadena, California 91125
(Received 28 June 1977)

We present calculations of the phononless Auger transition rates for excitons bound to the four common shallow acceptors (B, Al, Ga, and In) in Si and Ge. The calculated rates for the bound excitons in Si vary significantly for the different acceptors, increasing rapidly as the acceptor binding energy increases. This is in agreement with the rapid decrease with increasing acceptor binding energy of measured acceptor bound-exciton lifetimes in Si. Numerically, the calculated Auger rates are within about a factor of 3 of the measured recombination rates for the different acceptors. The dependence of the Auger rates on acceptor binding energy is due to an increased spreading in momentum space of the bound-exciton wave function. In Ge, the calculated Auger rates are orders of magnitude less than the measured free-exciton recombination rate in undoped Ge, suggesting that the phononless Auger transition is not important for acceptor bound excitons in Ge. This is consistent with the experimental observation that light doping with shallow acceptors has little effect on the lifetimes of photoexcited carriers at low temperatures in Ge; whereas, in Si the carrier lifetimes can be decreased by orders of magnitude. The principal difference between Si and Ge is that the acceptor binding energies are much greater in Si than they are in Ge.

I. INTRODUCTION

A bound exciton (BE) consists of three carriers (two holes and one electron for acceptor BE; two electrons and one hole for donor BE) bound to a charged impurity. Because in a BE three carriers are localized in the same region of space, an Auger transition, in which an electron recombines with a hole and the energy is carried off by the third carrier, can occur. Auger transitions are believed to limit the lifetimes of bound excitons in many cases.[1-5] Auger transitions have also been shown to be important in band-to-band recombination and carrier capture at a trap site.[4,5] These processes have been studied theoretically,[4,5] but to our knowledge, no quantitative calculations of BE Auger rates in semiconductors have been presented.

The bound-exciton lifetimes for the four common shallow acceptors in Si(B, Al, Ga, In) have recently been measured.[3] The BE lifetime was found to be significantly shorter than the free-exciton (FE) lifetime in undoped Si for each type of acceptor. The BE lifetime was strongly dependent on the type of acceptor, decreasing rapidly (at least a factor of 200 from Si:B to Si:In) as the acceptor binding energy increased. The lifetimes were interpreted as due to Auger transitions without phonon assistance. Qualitatively similar behavior has been observed for excitons bound to acceptors in GaP.[2] The lifetimes for the BE in GaP were also interpreted as limited by phononless Auger transitions.

Because the BE lifetimes are shorter than the FE lifetimes in undoped Si, the addition of small concentrations of shallow acceptors can greatly change the decay rate of photoexcited carriers in Si at low temperatures. For example, the free-exciton lifetime in undoped Si is 2.6 μsec.[6] If Si is doped with In at the 10^{15} cm^{-3} level (or greater), the lifetime of photoexcited carriers (low excitation) is reduced to less than 5 nsec.[3] This dramatic reduction in carrier lifetime is most likely due to capture of a FE at the impurity to form a BE (the cross section for this process has recently been shown to be very large for Si:In at temperatures less than 10 °K[7]) followed by Auger recombination of the BE. The rate limiting step in the process is the Auger recombination rate (for doping in the 10^{16} cm^{-3} or greater level and temperatures less than 10 °K).[7]

In contrast to Si, doping Ge with shallow acceptors at the 10^{15} cm^{-3} level has little effect on the lifetime of photoexcited carriers for temperature and excitation conditions at which electron-hole drops are not formed.[8,9] Both FE and BE are observed in the luminescence spectrum of Ge under these conditions and both decay with the lifetime of the FE in undoped Ge. Thus, it appears that Auger transitions for the BE in Ge are slow processes.

In this paper, we present calculations of the BE Auger rates for the common shallow acceptors in Si and Ge. The purpose of the calculation is to understand the strong dependence of the Auger rate on acceptor type in Si and the qualitatively different effect doping with shallow acceptors has on the lifetime of photoexcited carriers in Si and Ge. The result of the calculation shows the observed dependence of the BE lifetime on acceptor type in Si and is within about a factor of 3 of the measured lifetime in absolute value. The computed BE Auger rates in Ge are found to be much slower than the measured free-exciton lifetime in Ge. The impor-

tant difference in the two materials is that the holes are much more strongly bound to the acceptors in Si than they are in Ge.

The paper is organized in the following way: the qualitative physics of the Auger transition is discussed in Sec. II. In Sec. III, the calculation is presented, and the result of the calculation is compared with experiment. Our conclusions are given in Sec. IV. Calculational details are included in Appendix A. Appendix B contains a calculation of BE no-phonon oscillator strengths used to test the BE wave function used in the Auger calculation.

II. QUALITATIVE PHYSICS OF THE AUGER TRANSITIONS

In their work on GaP, Dean and co-workers argued that the dependence of acceptor BE lifetimes on acceptor type could be understood as due to an increased localization (hence, an increased spreading in K space) of the hole wave function in the BE for the more tightly bound acceptors.[2] (They did not, however, present quantitative calculations of the BE Auger rates to support their arguments.) We believe that the physical picture they suggest also applies to Si and can be used to understand the qualitatively different effect of doping with shallow acceptors on carrier lifetimes in photoexcited Si and Ge.

In the acceptor BE (initial state of the Auger transition) there are two holes near the valence-band maximum and an electron near the conduction-band minimum. The final state of the acceptor BE Auger transition has one hole in the valence band. The holes in the BE are spread in K space because they are localized about the acceptor. The electron state will also be spread in K space, but the spreading will be small compared to that of the holes because the electron is not localized as much as the holes. The wave vector of the final-state hole lies on a constant energy surface as required by energy conservation in the transition. Carrier-carrier scattering, which conserves total wave vector, is the dominant interaction responsible for an Auger transition. Thus, for the Auger transition to take place, the initial BE state must have an amplitude to contain wave vectors which are accessible to the final-state hole. The conduction-band minimum is rather far in K space from the constant energy surface of the final-state hole. Since the BE wave function is peaked at the conduction-band minimum, spreading of the BE wave function in K space is essential for the Auger transition to occur. In Si, the holes in the acceptor BE are well localized, resulting in large hole wave function spreading and fast Auger rates. The dependence on acceptor type occurs because the acceptors with larger binding energy bind the holes in the BE more tightly leading to faster Auger rates. In Ge, the holes in the acceptor BE are not tightly bound, so that the hole wave-function spreading is small and the Auger rates are slow.

In principle, the Auger transition could be phonon assisted. In contrast to the phononless Auger transition, an Auger transition involving a phonon should not be sensitive to the wave-function spreading in the BE because the phonon would make up the difference in wave vector between the peak in K space of the BE wave function and the final-state hole. As a result the phonon-assisted Auger transition rate should be insensitive to the acceptor type. Since the observed BE lifetimes in Si are, in fact, very sensitive to the acceptor type, the acceptor BE Auger transitions in Si most likely occur without phonon assistance. In Ge, it is very difficult to know whether the phonon-assisted or no-phonon Auger transition is more likely. Experimentally, neither process appears to be important. We will show that the no-phonon Auger process (which dominates in Si) is slow in Ge.

In order to compute the BE Auger rate, it is necessary to know the BE wave function. It is very difficult to compute this wave function accurately, and we use an idealized model. In particular, we describe the interaction of the holes with the charged acceptor by a Coulomb potential and a short-range square well. For Si:Al and Ge:Ga (the impurity has the same core structure as the host) the strength of the short-range well was taken to be due only to the wave-vector dependence of the dielectric function. For the other impurities, it was adjusted to produce the observed acceptor binding energies for a simple hydrogenic model of the acceptor. In order to check the approximate validity of the model BE wave function, we used it to compute no-phonon oscillator strengths for BE absorption. For Si:Al, Si:Ga, and Si:In the results are within a factor of 2 of the measured values.[10] For Si:B, the computed oscillator strength is about a factor of 4 too large. We readjusted the strength of the square wells so as to give wave functions which produce the measured oscillator strengths. This procedure is appropriate because both the no-phonon oscillator strength and the Auger transition rate depend sensitively on the extent of K-space spreading of the hole wave function and hence on the strength of the short-range potential. In contrast, the acceptor binding energy is not as strongly dependent on the strength of the short-range potential. For Ge, the computed oscillator strengths were so small that they are probably not observable. This is consistent with the lack of no-phonon BE optical transitions for Ge doped with acceptors, but is not of much help in the Auger rate calculations.

III. CALCULATION OF AUGER TRANSITION RATES

From time-dependent perturbation theory, the BE Auger transition rate is given by

$$\frac{1}{\tau}=\frac{2\pi}{\hbar}\sum_{F;\mathrm{Av}I}|\langle F|H|I\rangle|^2\delta(E_I-E_F)\ . \tag{1}$$

Here $|F\rangle$ is the final state which consists of a free hole, $|I\rangle$ is the BE initial state, and H is the Hamiltonian for the solid. (The states $|I\rangle$ and $|F\rangle$ are only approximate eigenstates of H.) The BE wave function has the form

$$|I\rangle=\sum_{k_h,k_h',k_e,m_1m_2}A^{JM}_{m_1m_2}(k_h,k_h',k_e)\,\Psi(k_hm_1;k_h'm_2;k_e\sigma_e), \tag{2}$$

where $\Psi(k_hm_1;k_h'm_2;k_e\sigma_e)$ is a Slater determinant with the valence-band states (k_hm_1) and $(k_h'm_2)$ empty and the conduction-band state $(k_e\sigma_e)$ occupied. Here m_1 and m_2 label the four hole bands degenerate at the valence-band maximum and σ_e labels the electron spin. For simplicity, we neglect valley orbit-splitting effects in the BE and restrict the electron to a particular conduction-band minimum. $A^{JM}_{m_1m_2}$ is the amplitude that a particular determinant is contained in the BE wave function; J is the total hole spin (2 or 0) with projection M along the Z axis. The final state is

$$|F\rangle=\Psi(k_f\sigma_f)\ , \tag{3}$$

where $\Psi(k_f\sigma_f)$ is a Slater determinant with the valence-band state $(k_f\sigma_f)$ empty and σ_f is the final-state hole spin. (We neglect spin-orbit splitting in the final state and the hole band index is included with σ_f.)

Using the wave functions given by Eqs. (2) and (3), the transition-matrix element becomes[11]

$$\begin{aligned}\langle F|H|I\rangle=\sum_{k_ek_hk_h'm_1m_2}&A^{JM}_{m_1m_2}(k_h,k_h',k_e)\\&\times(\langle\phi_{k_hm_1};\phi_{k_h'm_2}|V_{ee}|\phi_{k_f\sigma_f}\phi_{k_e\sigma_e}\rangle\\&-\langle\phi_{k_h'm_2};\phi_{k_hm_1}|V_{ee}|\phi_{k_f\sigma_f}\phi_{k_e\sigma_e}\rangle),\end{aligned} \tag{4}$$

where ϕ is a one-electron Bloch function and V_{ee} is the Coulomb interaction. The two-electron matrix elements in Eq. (4) can be written

$$\begin{aligned}&\langle\phi_{k_hm_1};\phi_{k_h'm_2}|V_{ee}|\phi_{k_f\sigma_f}\phi_{k_e\sigma_e}\rangle\\&=\sum_{GG'}U_{k_hm_1;k_f\sigma_f}(G)\,U_{k_h'm_2;k_e\sigma_e}(G')\\&\quad\times\frac{e^2(2\pi)^3\delta(\vec{k}_f+\vec{k}_e-\vec{k}_h-\vec{k}_h'+\vec{G}-\vec{G}')}{\epsilon(\vec{k}_f-\vec{k}_h+\vec{G})|\vec{k}_f-\vec{k}_h+\vec{G}|^2}\ .\end{aligned} \tag{5}$$

Here ϵ is the dielectric function, G and G' are reciprocal-lattice vectors, and

$$U_{k_hm;k\sigma}(G)=\frac{1}{\Omega}\int d^3r\,e^{-i\vec{G}\cdot\vec{r}}\,u_{k_hm}(r)u^*_{k\sigma}(r)\ , \tag{6}$$

where u is the periodic part of the Bloch function and Ω is the sample volume.

The maximum contribution to the matrix element comes from terms with $G=0$ so that the denominator can be small. The δ function in Eq. (5) requires that

$$\vec{k}_f+\vec{k}_e-\vec{k}_h-\vec{k}_h'+\vec{G}'=0 \tag{7}$$

for $G=0$. The amplitude function, A, will be peaked at $\vec{k}_h\sim\vec{k}_h'\sim0$ and $\vec{k}_e\sim\vec{k}_{e0}$ where k_{e0} is the conduction-band minimum. The wave vector $\vec{k}_f$ lies on a constant energy surface. For Si, $\vec{k}_{e0}$ is about 82% of the way out in the Brillouin zone in the [100] direction[12] and k_f is approximately 25% of the way out in the zone with the value varying somewhat with the direction of $\vec{k}_f$. Under these conditions, the most important term in the sum over $\vec{G}'$ will be with $\vec{G}'=0$. For Ge, $\vec{k}_{e0}$ is at the zone edge in the [111] direction so that there is a nonzero $\vec{G}'$ that puts $\vec{k}_{e0}+\vec{G}'$ at the zone edge in the $[\bar1\bar1\bar1]$ direction. Both this term and the one with $\vec{G}'=0$ will be significant in the sum on $\vec{G}'$. These two terms are important for different values of k_f so there is no interference between them, and they give the same contribution to the Auger rate. Thus, we evaluate the contribution to one of the terms and multiply this by a factor of 2. (Since our conclusion will be that the BE Auger rate in Ge is several orders of magnitude smaller than the measured free-exciton lifetime, this factor of 2 is not important.) Thus, for Si and Ge we need only consider the term $\vec{G}=\vec{G}'=0$ in Eq. (5).

The wave-function amplitude function is taken to have the form

$$A^{JM}_{m_1m_2}(k_h,k_h',k_e)=C^{JM}_{m_1m_2}f_h(k_h)f_h(k_h')f_e(k_e)\ , \tag{8}$$

where the coefficients C are chosen to give wave functions that are eigenstates of the total spin of the two holes. In particular, we have

$$C^{22}_{\frac32\frac12}=C^{21}_{\frac32-\frac12}=C^{2-1}_{\frac12-\frac32}=C^{2-2}_{\frac12-\frac32}=1 \tag{9a}$$

and

$$C^{20}_{\frac32-\frac32}=C^{20}_{\frac12-\frac12}=C^{00}_{\frac32-\frac32}=-C^{00}_{\frac12-\frac12}=\frac{1}{\sqrt2} \tag{9b}$$

and all others are zero. The BE wave function is properly normalized so long as the one-electron functions f_h and f_e are. Using this notation, Eq. (4) becomes

$$\langle F|H|I\rangle = \sum_{k_h k_h' k_e m_1 m_2} f_h(\vec{k}_h) f_h(\vec{k}_h') f_e(\vec{k}_e) U_{k_h m_1; k_f \sigma_f} U_{k_h m_2; k_e \sigma_e} \frac{e^2(2\pi)^3 \delta(\vec{k}_f + \vec{k}_e - \vec{k}_h - \vec{k}_h')}{\epsilon(\vec{k}_f - \vec{k}_h)|\vec{k}_f - \vec{k}_h|^2} (C^{JM}_{m_1 m_2} - C^{JM}_{m_2 m_1}) \ . \tag{10}$$

We next consider the overlap integrals U. Both k_f and k_h are toward the zone center and in the upper valence band. From the $\vec{k}\cdot\vec{p}$ calculations of Cardona and Pollak,[13] we see that overlap integrals of the form $U_{k_h m_1; k_f \sigma_f}$ are not strongly dependent on the magnitude of $\vec{k}_f$ or $\vec{k}_h$ in Si and Ge, and we make the approximation

$$U_{k_h m_1; k_f \sigma_f} \approx \lim_{k_f \to 0} U_{0 m_1; k_f \sigma_f} \ . \tag{11}$$

The value depends on m_1, σ_f, and the final-state hole band index b_f. An analogous approximation cannot be used for $U_{k_h' m_2; k_e \sigma_e}$ in Si because it is zero at $\vec{k}_h' = 0$ and $\vec{k}_e = \vec{k}_{e0}$. Since the spreading in K-space of the holes in the BE is much greater than that for the electron, we set $\vec{k}_e = \vec{k}_{e0}$ and expand in $\vec{k}\cdot\vec{p}$ perturbation theory for k_h' away from the zone center. Using the $\vec{k}\cdot\vec{p}$ perturbation theory, the periodic part of the hole Bloch function is

$$u_{k_h' m_2}(r) = u_{0 m_2}(r) + \frac{\hbar}{m} \sum_{b\sigma''} u_{0 b \sigma''}(r) \times \frac{\langle u_{0 b \sigma''} | \vec{k}_h' \cdot \vec{p} | u_{0 m_2} \rangle}{E_0 - E_b} \ , \tag{12}$$

where b labels bands and σ' spins. Then we have

$$U_{k_h' m_2; k_e \sigma_e} \approx \vec{k}_h' \cdot \vec{M}_{0 m_2; k_{e0} \sigma_e} \ , \tag{13a}$$

where

$$\vec{M}_{0 m_2; k_{e0} \sigma_e} = \frac{\hbar}{m} \sum_{b\sigma''} U_{0 b \sigma''; k_{e0} \sigma_e} \frac{\langle u_{0 b \sigma''} | \vec{p} | u_{0 m_2} \rangle}{E_0 - E_b} \ . \tag{13b}$$

The only band which makes a significant contribution to the sum in Eq. (13b) for Si is the Γ_{15} conduction band. If $\vec{k}_{e0}$ is taken to define the Z direction, the Z component of $\vec{M}$ is zero.

In Ge, $U_{0 m_2; k_{e0} \sigma_e}$ is not zero as it is in Si. However, the $\vec{k}\cdot\vec{p}$ calculations of Cardona and Pollak[13] show that this overlap integral is small. We have computed the Auger rates in Ge both approximating $U_{k_h m_2; k_e \sigma_e}$ by $U_{0 m_2; k_{e0} \sigma_e}$ and using the $\vec{k}\cdot\vec{p}$ expansion similar to Si (that is, setting $U_{0 m_2; k_{e0} \sigma_e}$ equal to zero). The second result gave almost an order of magnitude larger Auger rates. It is the one we report.[14] For Ge, the Γ_2' conduction band makes the dominant contribution to the sum in Eq. (13b).

With these approximations, the transition-matrix element becomes

$$\langle F|H|I\rangle = \sum_{m_1 m_2} (C^{JM}_{m_1 m_2} - C^{JM}_{m_2 m_1}) \times U_{0 m_1; b_f \sigma_f} \vec{M}_{0 m_2; k_{e0} \sigma_e} \cdot \vec{\beta}(\vec{k}_f) \ , \tag{14a}$$

where

$$\vec{\beta}(\vec{k}_f) = \left(\frac{1}{2\pi}\right)^3 \frac{1}{2\pi^2} \int d^3k_h \, d^3k_h' \, f_h(\vec{k}_h) f_h(\vec{k}_h') \times f_e(\vec{k}_h + \vec{k}_h' - \vec{k}_f) \times \frac{e^2 \vec{k}_h'}{\epsilon(\vec{k}_h - \vec{k}_f)|\vec{k}_h - \vec{k}_f|^2} \ . \tag{14b}$$

To obtain the transition rate, the matrix element is squared, averaged over the initial BE states and summed over final states. The most important final hole states are in the two upper valence bands; these two bands are degenerate in the [100] and [111] directions. We include only these two bands in the summation and neglect the fact that they are not degenerate in all directions.[15] The remaining summations on discrete indices can be performed in a straightforward but tedious way. The result becomes

$$1/\tau = |D|^2 B \ , \tag{15a}$$

where

$$|D|^2 = [2](\tfrac{2}{3})^2 |\langle u_\Gamma | u_c \rangle|^2 \left(\frac{\hbar}{m}\right)^2 \frac{|\langle u_\Gamma | p_x | u_{\Gamma_{25'}} \rangle|^2}{(E_\Gamma)^2} \tag{15b}$$

and

$$B = \frac{2\pi}{\hbar} \frac{1}{(2\pi)^3} \int d^3k_f \, \beta_x^2(\vec{k}_f) \delta(E_I - E_F) \ . \tag{15c}$$

The factor of 2 in square brackets is to the included for Ge but not for Si. In Eq. (15), Γ refers to the Γ_{15} conduction-band state for Si and the Γ_2' conduction-band state for Ge; c refers to the conduction-band minimum (Δ_1 in Si and L_1 in Ge) and p_x is the x component of the momentum operator. (The minimum of the conduction band is taken to define the Z axis; the x and y components which appear in the product $\vec{M}\cdot\vec{\beta}$ give equal contributions to the transition rate.)

To evaluate $\vec{\beta}(\vec{k}_f)$, it is necessary to obtain the envelope functions $f_h(\vec{k}_f)$ and $f_e(\vec{k}_e)$. As a first approximation, we use effective-mass theory with a simplified model for the band structure. The electron effective mass is taken to be spherical with a value[16]

$$1/m_e = \tfrac{1}{3}(2/m_t + 1/m_e) \ , \tag{16}$$

where m_t is the transverse electron effective mass and m_e is the longitudinal electron effective mass. The interaction between the holes and the charged acceptor is taken to be a Coulomb part, screened by the static dielectric function, plus a short-range square well. The radius of the square well

is taken to be the covalent radius of the host. For Si: Al and Ge:Ga (the impurity with the same core structure as the host), the square well is taken to be due only to the dielectric function. In Appendix A, we obtain an expression for the depth of square well for Si: Al and Ge: Ga based on this assumption. The hole effective mass is taken to be spherical. We chose a value for the hole effective mass by making a variational calculation for the Si: Al and Ge: Ga acceptors, using a 1s hydrogenic wave function and fitting the measured binding energy. For impurities other than Al in Si and Ga in Ge, we determine the depth of the square well by making a variational calculation for the acceptor using a 1s hydrogenic wave function and fitting the measured binding energy. The interaction between the electron and the charged acceptor was taken to be the same as for holes but with the sign changed.

As a first approximation, f_h and f_e are assumed to have a 1s hydrogenic form

$$f_h(k)=\left(\frac{\pi}{a^5}\right)^{1/2}\frac{8}{[k^2+(1/a)^2]^2}, \tag{17a}$$

$$f_e(k)=\left(\frac{\pi}{b^5}\right)^{1/2}\frac{8}{[k^2+(1/b)^2]^2}. \tag{17b}$$

The Bohr radii for the holes and electrons are determined from a variational calculation.

There are corrections to the effective-mass approximation for wave vectors far from the band extrema because the hole dispersion curves are not parabolic at large $\vec{k}$. We take these corrections into account by substituting the hydrogenic form into the Hartree equation for the holes in the BE

$$f_h(k)=\frac{1}{E(k)+E_B}\sum_{k'}V_{kk'}f_h^H(k'). \tag{18}$$

Here $E(k)$ is the hole dispersion curve, E_B is the one hole Hartree energy, f_h^H is the hydrogenic form for the hole wave function [Eq. (17a)] and V is the Hartree potential seen by the hole computed taking the hydrogenic forms for the envelope function

$$V(r)=\frac{-e^2}{\epsilon(0)r}+\frac{e^2}{\epsilon(0)}\times\int\frac{|f_h^H(r')|^2}{|r-r'|}d^3r'\frac{-e^2}{\epsilon(0)}\times\int\frac{|f_e^H(r')|^2}{|r-r'|}d^3r'\frac{-4\pi}{3}V_0R^3\delta(r). \tag{19}$$

Here the short-range square well of radius R and depth V_0 has been replaced by a δ function for convenience. (The Fourier transform of the square well is effectively constant for the range of wave vectors of interest.) Evaluating the integrals using the hydrogenic functions and using the fact that the hole Bohr radius is much smaller than the electron Bohr radius gives

$$V(r)\simeq\frac{-e^2}{\epsilon(0)}e^{-2r/a}\left(\frac{1}{r}+\frac{1}{a}\right)\frac{-4\pi}{3}V_0R^3\delta(r). \tag{20}$$

Using this form for the potential, the iterated wave function is

$$f_h(k)=\frac{e^2}{\epsilon(0)}\frac{4\pi}{(\pi a^3)^{1/2}}\frac{1}{E(k)+E_B}\times\left(\frac{1}{k^2+9/a^2}+\frac{6}{a^2(k^2+9/a^2)^2}+\frac{V_0R^3}{6e^2/\epsilon(0)}\right). \tag{21}$$

Although this function appears to be quite different than the hydrogenic form, they are numerically rather close at small $\vec{k}$. At large $\vec{k}$, where both functions are small, the iterated functions dies off more slowly with increasing $\vec{k}$ than the hydrogenic form. We compare the two functions for $\vec{k}$ in the [111] direction for Si: Ga in Fig. 1.[17] (Si: Ga represents a case with an intermediate value for the strength of the short range potential. The [111] direction is the one of greatest interest because the hole dispersion curves for Si and Ge drop off most slowly in this direction so that the hole wave function is spread most effectively in this direction.) In the calculations of Auger rates and no-phonon oscillator strengths, we will only need the

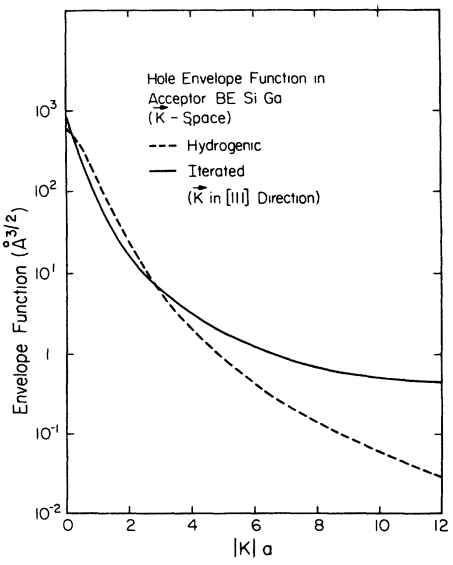

FIG. 1. Hole envelope function for the BE in Si:Ga vs wave vector in units of the hole Bohr radius. The dashed line is the hydrogenic form for the envelope function [see Eq. (17a)] and the solid line is the iterated form [see Eq. (21)]. The wave vector is in the [111] direction; $|K|a=12$ corresponds to the zone edge.

TABLE I. No-phonon oscillator strengths for acceptor BE in Si.

	Measured	Calculated
Si:B	$\sim 2\times10^{-6}$ [a,b]	8.7×10^{-6}
Si:Al	7×10^{-6} [a]	3.5×10^{-6}
Si:Ga	1×10^{-5} [a]	9.0×10^{-6}
Si:In	9×10^{-5} [a]	9.3×10^{-5}

[a] Reference 10.

[b] Estimated from the measured TO-phonon oscillator strength of Ref. 10 and the ratio of TO to no-phonon emission intensity given by R. Sauer and J. Weber [Phys. Rev. Lett. 36, 48 (1976)].

iterated form of the hole wave function in the tail region.

In order to test the validity of the BE wave function, we have used this function to compute no-phonon oscillator strengths for acceptor BE in Si and Ge. The details of this calculation are given in Appendix B. In Ge, the acceptor BE no-phonon optical transitions are too weak to observe.[18] Our calculation produces very small oscillator strengths[19]; this is consistent with experiment, but not very helpful. In Si, the acceptor BE no-phonon oscillator strengths have been measured.[10] In Table I, we list the measured oscillator strengths and the computed values for Si. For Si:Al, Si:Ga and Si:In, the results are within about a factor of 2 of the measured values; for Si:B, the calculated oscillator strength is about a factor of 4 too large. Si:B is different than the other cases because the square-well potential is repulsive for holes in this case. The binding energy for the acceptor is not very sensitive to the strength of this potential; the no-phonon oscillator strength is rather sensitive to it. In addition, the no-phonon oscillator strength is sensitive to the tail (in K space) of the hole wave function in much the same way as the Auger transition rate. We adjust the depth of the square-well potential to produce the measured oscillator strength. This adjustment is most significant for Si:B, if we had not made the adjustment, the calculated Auger rate for Si:B would be about a factor of 3 larger than that which we report.

In Table II, we list the square-well parameters and resulting Bohr radii determined by the acceptor binding energy and by the no-phonon oscillator strengths. We also list the acceptor binding energies produced by the square wells determined by the no-phonon oscillator strengths. In Si:B, the strength of the repulsive square well is reduced to produce the measured oscillator strengths, and as a result the corresponding acceptor binding energy is greater than the measured value.

With the approximate expressions for the envelope functions, f_h and f_e, we can perform the integral in Eq. (14b). First, we note that the function f_e is much more sharply peaked than the other function (the electron Bohr radius is large) and replace it by a normalized δ function,

$$f_e(\vec{k}_e)\approx[(2\pi)^3/(\pi b^3)^{1/2}]\delta(\vec{k}_e-\vec{k}_{e0}). \tag{22}$$

Then we have

$$\vec{\beta}(\vec{k}_f)=\frac{1}{2\pi^2}e^2\frac{1}{(\pi b^3)^{1/2}}\int d^3k_h\,\frac{f_h(\vec{k}_h)f_h(\vec{k}_{e0}+\vec{k}_f-\vec{k}_h)(\vec{k}_f+\vec{k}_{e0}-\vec{k}_h)}{\epsilon(\vec{k}_h-\vec{k}_f)\,|\vec{k}_h-\vec{k}_f|^2}. \tag{23}$$

The calculation would still be very lengthy if it was done without further simplicifation because both the integration in $\vec{\beta}(\vec{k}_f)$ and the final-state integration $\vec{k}_f$ involve evaluation of valence-band energies at every point. We have examined the integration in Eq. (23) numerically and found that nearly all the contribution to the integral comes from the region near $\vec{k}_h=0$. This occurs because the function $f_h(\vec{k}_h)$ is peaked at $\vec{k}_h=0$. There is no corresponding contribution at $(\vec{k}_{e0}+\vec{k}_f=\vec{k}_h)$ because

TABLE II. Square-well parameters and Bohr radii for acceptor BE in Si. The diameter of the square well is taken as the covalent radius of Si (1.11 Å). The unprimed numbers are determined by fitting acceptor binding energies and the primed numbers are determined by fitting no-phonon oscillator strengths.

	V_0R^3 (eV Å^3)	E_A (meV)	a (Å)	b (Å)	$V_0'R^3$ (eV Å^3)	E_A' (meV)	a' (Å)	b' (Å)
Si:B	−27.1	46	18.7	51.5	−12.0	53	16.4	48.2
Si:Al	2.8	67	13.0	43.3	4.9	70	12.4	42.5
Si:Ga	5.7	71	12.2	42.1	6.2	72	12.0	41.9
Si:In	14.8	154	7.7	34.9	14.8	154	7.7	34.9

of the factor $(\vec{k}_f+\vec{k}_{e0}-\vec{k}_h)$ and because the denominator $|\vec{k}_h-\vec{k}_f|^2$ is large in this region. As long as $a|\vec{k}_{e0}+\vec{k}_f|$ is much larger than unity, the integral in Eq. (23) is that of a sharply peaked function times a smoothly varying one in the region which contributes. In this case, the sharply peaked function can be reasonably approximated by a normalized δ function. Since we are only concerned with the part of $f_h(\vec{k}_h)$ where the function is large (i.e., near $\vec{k}_h=0$) we use the hydrogenic form to determine the normalization.

$$f_h(k_h)\approx[(2\pi)^3/(\pi a^3)^{1/2}]\delta(\vec{k}_h)\,. \tag{24}$$

To check the validity of this approximation, we have used it for the integral with $f_h(\vec{k}_{e0}+\vec{k}_f-\vec{k}_h)$ being hydrogenic. For the hole Bohr radius parameters used here the approximate result was within 50% of the exact value determined by numerical integration for all cases except Si: In. For Si: In the approximate result was within a factor of 2 of the exact result. When Eq. (21) is used for $f_h(\vec{k}_{e0}+\vec{k}_f-\vec{k}_h)$, the approximation should be better than for the hydrogenic form because $f_h(\vec{k}_{e0}+\vec{k}_f-\vec{k}_h)$ is more slowly varying near $\vec{k}_h=0$ in this case. With this approximation, we have

$$\beta(\vec{k}_f)=\left(\frac{e^2}{2\epsilon(0)a}\right)^2\frac{64\sqrt{\pi a}}{ak_f}\left(\frac{a}{b}\right)^{3/2}(\vec{k}_{e0}+\vec{k}_f)\;\frac{1}{E(\vec{k}_{e0}+\vec{k}_f)+E_B}\;\frac{\epsilon(0)}{\epsilon(\vec{k}_h-\vec{k}_f)}$$
$$\times\left(\frac{1}{|\vec{k}_{e0}+\vec{k}_f|^2a^2+9}+\frac{6}{(|\vec{k}_{e0}+\vec{k}_f|^2a^2+9)^2}+\frac{V_0R^3}{6[e^2/2\epsilon(0)a]a^3}\right) \tag{25}$$

Here E_B is negligible compared to $E(\vec{k}_{e0}+\vec{k}_f)$; thus, it plays no role in the calculation of Auger rates.

The final-state integral in Eq. (15c) is performed numerically. The valence-band structure was obtained from a tight-binding band-structure calculation using essentially the parameters of Chadi and Cohen.[20] We have changed the second-nearest-neighbor interaction parameter (u_{xx} in the notation of Ref. 20) by 0.21 eV in Si and 0.16 eV in Ge in order to produce the known energies at the L_3 valence-band points.[21] It is desirable to get this point as accurately as possible because the largest contribution to the density of final hole states for the Auger transition in Si and Ge come with $\vec{k}$ in the [111] directions. In Table III, we list parameters used in the calculation.

In Fig. 2 we show the result of the calculation for Si along with experimental bound-exciton lifetimes for the four common shallow acceptors.[3,22] The calculated lifetimes show the same dependence on acceptor type as the observed lifetimes and have numerical values that differ by about a factor of 3 from the experimental lifetimes. Considering the simplified BE wave functions used in the calculation, we consider this agreement between the calculated Auger rates and measured lifetimes to be quite reasonable. The results indicate that the BE lifetimes are limited by phononless Auger transitions for acceptors in Si.

In Ge, it is difficult to determine the appropriate square-well parameters because the no-phonon acceptor BE oscillator strengths are so weak that these optical transitions have not been observed. In addition, the acceptor binding energies for the different acceptors are nearly the same in Ge, and they are not very sensitive to a short-range potential (due to the large Bohr radii of the acceptors in Ge). In Fig. 3, we plot calculated Auger rates for acceptor BE in Ge versus the square-well parameter V_0R^3. In the lower panel of the figure, we show the electron and hole Bohr radii. The range of the square-well parameter shown in the figure is over four times that used for Si: In. (The binding energy of the Ge: In acceptor is produced by a well parameter of 37 eV Å^3.) Over the entire range of the square-well parameters, the calculated Auger rate is almost two order of magnitude (or more) slower than the measured FE recombination rate in Ge. (The measured FE lifetime in undoped Ge is about 8 μsec.[23]) Since it seems unreasonable that the appropriate square-well depth for the shallow acceptors in Ge should be many times larger than that for Si: In, the calculation indicates that the phononless Auger rate for acceptor BE in Ge is too slow to significantly

TABLE III. Parameters used in the calculation. All symbols are defined in the text.

	Si	Ge
R	1.11 Å	1.22 Å
m_e	$0.26m$	$0.12m$
m_h	$0.60m$	$0.19m$
$\langle u_\Gamma\|u_c\rangle$	0.8 [a]	0.6 [a]
$\|\langle u_\Gamma\|P_x\|u_{\Gamma_{25'}}\rangle\|$	0.53 a.u. [a]	0.68 a.u. [a]
E_Γ	3.4 eV [a]	1.0 eV [a]
$\|\langle u_{\Delta_5}\|P_y\|u_{\Delta_1}\rangle\|$	0.57 a.u. [a]	...
$\|\langle u_{\Lambda_3}\|P_y\|u_{\Lambda_1}\rangle\|$	...	0.65 a.u. [a]

[a] Reference 13.

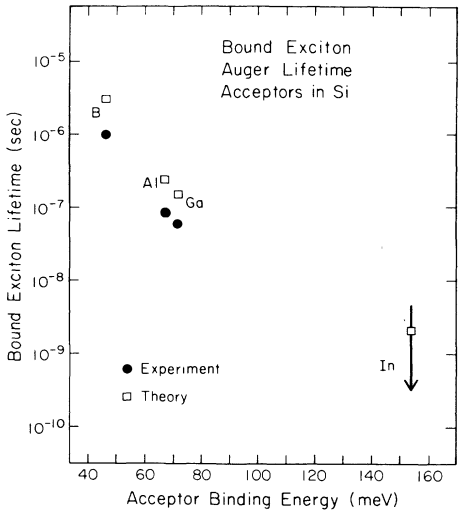

FIG. 2. Bound-exciton lifetimes vs impurity binding energy for the four common acceptors in Si. The hollow squares are our calculations of the Auger lifetime and the solid circles are the measure values from Ref. 3. Only an upper bound of 5 nsec (indicated by the top of the arrow) was set on the BE lifetime for Si:In in Ref. 3.

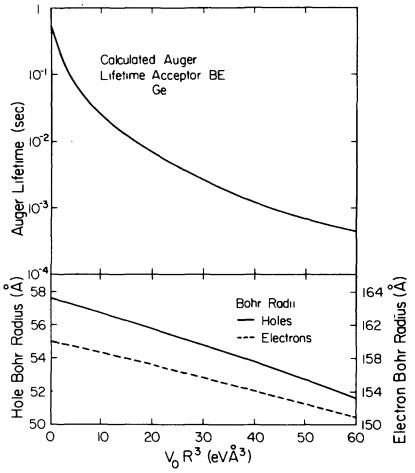

FIG. 3. Calculated Auger lifetimes for acceptor BE in Ge vs the square-well parameter V_0R^3. The range of square-well parameter is over four times that appropriate for Si:In. Even for this unrealistically large value, the calculated no-phonon Auger lifetime is almost two orders of magnitude greater than the measured FE lifetime in Ge indicating that the phononless Auger transition is not an important process for acceptor BE in Ge. In the lower panel, the hole and electron Bohr radii are shown.

influence the BE lifetime.[24] The slow Auger rates in Ge follow from the large Bohr radii.

IV. SUMMARY AND CONCLUSION

We have presented a calculation of phononless Auger transition rates for excitons bound to shallow acceptors in Si and Ge. We used a simplified model for the BE wave function and did not expect to produce numerically precise results (It would be a very formidable task to calculate a high-precision BE wave function. It would be necessary to include the degenerate valence-band structure, conduction-band anisotropies, and a realistic impurity-carrier potential in a three-body problem.) The purpose of the calculation was to understand the very large (almost three orders of magnitude) dependence of acceptor BE lifetimes observed in Si,[3] and the fact that shallow acceptors do not significantly effect the lifetime of photoexcited carriers in Ge at low temperature[8] (qualitatively different behavior than in Si). These are large effects and qualitative differences which can be accounted for in an approximate calculation.

The results of the calculation produced the strong dependence of the Auger rate on acceptor type for BE in Si. The calculated results deviated from the measured BE lifetimes by about a factor of 3. For Ge, the calculation gave Auger rates at least two orders of magnitude slower than the observed FE recombination rate in undoped Ge. We conclude that phononless Auger transitions limit the acceptor BE lifetime in Si, but are ineffective in Ge. The principal difference between the two materials is that the holes are much more tightly bound to the charged acceptor in Si than in Ge. Because the holes are more tightly bound in the Si BE, the hole wave function is more strongly spread in K space and the Auger rates are faster. This effect enters the calculation primarily through the hole Bohr radii which are much smaller in Si than in Ge. The increased spreading in K space for more tightly bound acceptors also accounts for the dependence of the Auger rate on acceptor type observed in Si.

ACKNOWLEDGMENTS

We thank S. A. Lyon, M. Chen, K. R. Elliott, D. S. Pan, J. N. Schulman, and T. C. McGill for valuable discussion on subjects related to this work. We thank P. J. Dean for drawing our attention to Ref. 2.

APPENDIX A: DIELECTRIC-FUNCTION CONTRIBUTION TO SHORT-RANGE POTENTIAL

In this appendix, we estimate the contribution to the short-range potential due to the frequency dependence of the dielectric function. We set the integrated value of the short-range potential equal to that for a square well,

$$\frac{4\pi}{3} V_0 R^3 = \int V_s(r)\, d^3r = V_s(q=0)\,. \tag{26}$$

For the short-range potential, we take

$$V_s(q) = (4\pi e^2/q^2)[1/\epsilon(q) - 1/\epsilon(0)]\,. \tag{27}$$

We use the form of $\epsilon(q)$ suggested by Nara and Morita[25] for Si; this gives 2.83 eV Å for V_0R^3.

For Ge, we use the same form for the dielectric function as in Si, but replace $\epsilon(0)$ with the measured value for Ge, 15.36. This form is a reasonable parametrization of the dielectric function calculation in Ge by Brust.[26] For Ge, we have $V_0R^3 = 2.89$ eV Å^3.

APPENDIX B: NO-PHONON OSCILLATOR STRENGTHS

In this appendix, we use the BE wave function to compute the no-phonon oscillator strengths for acceptor BE. The oscillator strength is defined as

$$f = (2/\hbar\omega m)\,|\langle I|P_y|F\rangle|^2\,. \tag{28}$$

Here $|F\rangle$ is the final-state acceptor BE, $|I\rangle$ is the initial-state acceptor, P is the momentum operator, and $\hbar\omega$ is the photon energy required in the optical transition; Eq. (28) is to be averaged over the initial acceptor states and summed over the final BE states. Using the BE wave function in Eq. (8) and an acceptor wave function of the form

$$|I\rangle = \sum_k F_m(k)\Psi(km)\,. \tag{29}$$

The matrix element can be written

$$\langle I|P_y|F\rangle = \sum_{k_h k_h'} \sum_{m_1 m_2 \sigma_e} f_h(\vec{k}_h) f_h(\vec{k}_h') f_e(\vec{k}_h) F_{m_2}(\vec{k}_h') \langle u_{k_h m_1}|P_y|u_{k_h \sigma_e}\rangle (C^{JM}_{m_1 m_2} - C^{JM}_{m_2 m_1})\,. \tag{30}$$

Here $u_{k_h\sigma_e}$ is the periodic part of the electron Bloch function and $u_{k_h m_1}$ is the periodic part of the hole Bloch function. We assume that the acceptor envelope function $F(\vec{k}_h')$ does not depend on the hole spin state m_2 and that near $\vec{k}_h = 0$ where $F(\vec{k}_h)$ and $f_h(\vec{k}_h)$ are large, they may be reasonably approximated by hydrogenic functions with Bohr radii a_A and a, respectively. In this case we have

$$\sum_{k_h'} f_h(\vec{k}_h') F_{m_2}(k_h') = \frac{8}{(1 + a_A/a)^3}\left(\frac{a_A}{a}\right)^{3/2}. \tag{31}$$

Next we use the fact that the spread of the electron envelope function in K space is very small compared to that for holes and replace $f_e(\vec{k}_h)$ with the normalized δ function given in Eq. (22). The matrix element becomes

$$\langle I|P_y|F\rangle = f_h(k_{e0}) \frac{1}{(\pi b^3)^{1/2}} \frac{8}{(1 + a_A/a)^3}\left(\frac{a_A}{a}\right)^{3/2} \times \sum_{m_1 m_2 \sigma} \langle u_{k_{e0} m_1}|P_y|u_{k_{e0}\sigma_e}\rangle \times (C^{JM}_{m_1 m_2} - C^{JM}_{m_2 m_1})\,. \tag{32}$$

The spin sums in Eq. (32), initial-state averages, and final-state sum can be performed in a straightforward but tedious way. In Si, the result is

$$f = \frac{2}{\hbar\omega m}\,|\langle u_{\Delta_5}|P_y|u_{\Delta_1}\rangle|^2 \times 4\left[\frac{8}{(1 + a_A/a)^3}\left(\frac{a_A}{a}\right)^{3/2}\right]^2 \left(\frac{f_h(\vec{k}_{e0})}{(\pi b^3)^{1/2}}\right)^2. \tag{33}$$

Here u_{Δ_5} is the periodic part of the hole Bloch function in the Δ_5 valence band at $\vec{k}_{e0}$ and u_{Δ_1} is the periodic part of the electron Bloch function at this point. The conduction-band minimum is in the z direction (a [100] direction).

For Ge, the result is

$$f = \frac{2}{\hbar\omega m}\,|\langle u_{\Lambda_3}|P_y|u_{\Lambda_1}\rangle|^2 \times \frac{8}{3}\left[\frac{8}{(1 + a_A/a)^3}\left(\frac{a_A}{a}\right)^{3/2}\right]^2 \left|\frac{f_h(\vec{k}_{e0})}{(\pi b^3)^{1/2}}\right|^2. \tag{34}$$

Here u_{Λ_3} and u_{Λ_1} are periodic parts of the hole and electron Bloch functions at the conduction-band minimum. The conduction-band minimum is in the z direction (a [111] direction).

*Work supported in part by AFOSR under Grant No. 77-3216.

[1]D. F. Nelson, J. D. Cuthbert, P. J. Dean, and G. D. Thomas, Phys. Rev. Lett. 17, 1262 (1962).
[2]P. J. Dean, R. A. Faulkner, S. Kimura, and M. Ilegems, Phys. Rev. B 4, 1926 (1971).
[3]S. A. Lyon, G. C. Osbourn, D. L. Smith, and T. C. McGill, Solid State Commun. 23, 425 (1977).
[4]P. T. Landsberg, Phys. Status Solidi 41, 457 (1970).
[5]P. T. Landsberg and M. J. Adams, J. Lumin. 7, 3 (1973).
[6]J. D. Cuthbert, Phys. Rev. B 1, 1552 (1970).
[7]K. R. Elliott, D. L. Smith, and T. C. McGill (unpublished).
[8]M. Chen, D. L. Smith, and T. C. McGill, Phys. Rev. B 10, 4983 (1977).
[9]At temperatures and excitation conditions for which electron-hole drops are formed, the decay of the drops is slower in lightly doped Ge than in undoped Ge. This effect can be understood as due to a reduction

in the exciton diffusion away from the drops resulting in slower net evaporation of carriers [M. Chen, S. A. Lyon, K. R. Elliott, D. L. Smith, and T. C. McGill, Nuovo Cimento B 39, 622 (1977)]. At doping levels of 10^{16} cm^{-3} or greater, the luminescence spectrum of Ge at low temperatures is complicated and shows complicated decay transients (see Ref. 8); however, the decay is slower than in pure Ge. This behavior is qualitatively different than in Si.

[10]P. J. Dean, W. F. Flood, and G. Kaminsky, Phys. Rev. 163, 721 (1967).

[11]We have dropped a term in Eq. (4) which corresponds to interband scattering by the impurity potential. This term makes a negligible contribution to the Auger transition rate for two reasons: first, it depends on the small expansion of a hole orbital going from the acceptor to the BE; second, the lowest-order term in the $\vec{k}\cdot\vec{p}$ expansion [see Eq. (12)] does not contribute to this term.

[12]W. P. Dumke, Phys. Rev. 118, 938 (1960).

[13]M. Cardona and F. H. Pollak, Phys. Rev. 142, 530 (1966).

[14]In Ref. 13, $\langle u_{\Gamma_{25}'}|u_{L_1}\rangle$ is found to be about 0.1; whereas, $\langle u_{\Gamma_{15}}|u_{L_1}\rangle$ is about 0.6. These overlap integrals are squared in the Auger rates. Because the overlap which appears in the first-order $\vec{k}\cdot\vec{p}$ expansion is considerably larger than that which appears in the zeroth-order term, the first-order term dominates. If these two overlap integrals were comparable, the zeroth-order term would be the more important.

[15]When performing the final state integration over k_f, we integrated over both bands and averaged the result. The integrations for the two bands differed by about 50%.

[16]W. F. Brinkman and T. M. Rice, Phys. Rev. B 7, 1508 (1973).

[17]In Fig. 1, we estimate the hole Hartree energy by the BE dissociation energy. This energy only effects the iterated wave function illustrated in Fig. 1 for $|K|a \lesssim 0.5$ and does not come into the actual Auger calculation at all since we use the hydrogenic form in the small-$|K|$ region.

[18]E. F. Gross, B. V. Nokikov, and N. S. Sokolov, Fiz. Tverd. Tela. 14, 443 (1972) [Sov. Phys.-Solid State 14, 368 (1972)].

[19]We compute a no-phonon oscillator strength of 2×10^{-7} for a square well parameter (V_0R^3) of 37 eV Å^3 which produces the Ge:In acceptor binding energy. This is about an order of magnitude smaller than the weak no-phonon oscillator strength in Si:B. The calculated oscillator strengths for square-well parameters which produce the binding energies for the other acceptors in Ge are much less than that for Ge:In. The calculated no-phonon oscillator strengths in Ge are small because the hole Bohr radii are large.

[20]D. J. Chadi and M. L. Cohen, Phys. Status Solidi B 68, 405 (1975).

[21]See, for example, J. C. Phillips, Solid State Phys. 18, 55 (1966).

[22]In Ref. 3, the measured lifetime for the BE in Si:Al was reported to be 104 nsec. Following discussions with M. H. Pilkuhn and W. Schmid, the BE lifetime in Si:Al was remeasured using lower excitation intensity. The lifetime decreased slightly to 80 nsec suggesting that there was saturation of the Al impurities in the earlier measurement. Lifetimes for the other impurities showed no change (higher doping levels were used for the other impurities). [S. A. Lyon (private communication)].

[23]Ya. Pokrovskii, Phys. Status Solidi A 11, 385 (1972).

[24]Except at very low temperatures, excitons probably ionize rapidly from shallow acceptors in Ge because the dissociation energy is only about 1 meV (see Ref. 18). Thus, unless the acceptor BE has decay channels available to it (such as an Auger transition) which are rapid compared to the processes responsible for FE decay both the BE and FE densities will decay at a rate governed by the processes responsible for FE decay. At temperatures low enough that dissociation of the BE in Ge is slow compared to the FE lifetime (probably less than 2 °K) photoexcited carriers in Ge form electron-hole drops.

[25]H. Nara and A. Morita, J. Phys. Soc. Jpn. 21, 1852 (1966).

[26]D. Brust, Phys. Rev. B 5, 435 (1972).